Beam-plasma coupling effects on the stopping power of dense plasmas

D. O. Gericke and M. Schlanges
Institut für Physik, Ernst-Moritz-Arndt Universität Greifswald, Domstrasse 10a, 17487 Greifswald, Germany
(Received 18 December 1998)

The stopping power for ion beams in dense plasmas is investigated on the basis of quantum kinetic equations. Strong correlations between the beam ions and the plasma particles which occur for high ion charge numbers and strongly coupled plasmas are treated on the level of the statically screened *T*-matrix (binary collision) approximation. Dynamic screening effects are included using a combined scheme which considers both close collisions and collective effects. Applying this approach, the ion charge number dependence of the stopping power is determined. The result is a modification of the Z_b^2 scaling law. In particular, the stopping power is reduced for strong beam-plasma coupling. Good agreement is found between *T*-matrix results and simulation data (particle-in-cell and molecular dynamics) for low beam velocities. [S1063-651X(99)09607-5]

PACS number(s): 52.25.Fi, 52.25.Ub, 52.40.Mj

I. INTRODUCTION

The stopping power is an important quantity to describe the interaction of particle beams with matter. In the field of particle driven inertial confinement fusion, the interaction of highly charged ions with dense plasmas is of special interest [1–3]. Both in the indirect driven scheme where the fast ions heat up a converter and in direct ion beam-fusion core interaction, strong beam-plasma coupling effects occur. These effects are caused by the high ion charge number in plasmas [4] and the high carrier densities in the target. Furthermore, stopping power data are needed to model the cooling of beams of highly charged ions in electron cooling devices [5]. Due to the high charge states of the ions, the low temperature of the electron gas, and the small relative velocity between ions and electrons, one also has to consider strong beam-plasma coupling effects in such devices.

In the case of very slow ions and classical plasmas, the coupling strength between the beam ions and the free plasma electrons, which give the main contribution to the stopping power in highly ionized plasmas, can be described by the parameter $Z_b\Gamma$. Here Z_b is the beam charge number (the subscript *b* labels the beam particle), and Γ is the nonideality parameter of the electron gas defined by the ratio of the Landau length $l=e^2/k_BT$ and the mean interparticle distance $\overline{r}=(4\pi n/3)^{-1/3}$, i.e.,

$$\Gamma = e^2(4\pi n/3)^{1/3}/k_BT. \tag{1}$$

For larger beam velocities, the kinetic energy of the plasma electrons has to be replaced by the mean kinetic energy of relative motion $E=\frac{1}{2}m_e\langle v_r^2\rangle$, where v_r is the velocity of ion-electron relative motion. Of course, this leads to a reduction of the coupling strength for higher beam velocities. A further important parameter to characterize the beam-plasma interaction is the Coulomb parameter η defined as

$$\eta = \frac{|Z_b|e^2}{\hbar\langle v_r\rangle}. \tag{2}$$

For $\eta \gg 1$ a classical treatment can be applied, whereas in the case of $\eta < 1$, e.g., for high beam velocities, quantum effects have to be considered. Interestingly, the parameter η also gives an estimate for the beam-plasma coupling strength [6]. It follows that strong correlations are expected to be significant in the classical region $\eta \gg 1$. Furthermore, the parameter $\kappa\lambda$, with an inverse screening length $\kappa = 4\pi e^2 \Sigma_c n_c/k_BT$ and a thermal wavelength $\lambda = \sqrt{\hbar^2/m_e k_B T}$, has to be considered because only in the case of $\kappa\lambda \ll 1$ can classical calculations be applied.

Of course, strong beam-plasma coupling effects cannot be treated in the framework of Born-type approximations as in the case of the linear response theory using the dielectric function in the random phase approximation (RPA) [7]. Such weak coupling theories predict an increase of the stopping power according to a Z_b^2 scaling law. Deviations from this scaling were found by Barkas and co-workers [8]. In more recent experiments with electron cooling devices, a Z_b^x scaling with $x=1.5$–1.7 could be obtained for the stopping power [5,9]. There exist different theoretical attempts to interpret these results. Using perturbation theory, Z_b^3 corrections to the stopping power were calculated [10]. Furthermore, the stopping of antiprotons in an electron gas corresponding to metallic densities was investigated in a scheme where the scattering quantities were calculated within a phase shift approach [11,12]. Here the beam-plasma interaction potential was determined self-consistently by density functional theory considering effects of screening nonlinearity. A more general approach for the low velocity limit is given in Ref. [13] in terms of the force autocorrelation function. On the other hand, simulation techniques such as molecular dynamics simulations [14,15] and calculations dealing with the nonlinearized Vlassow-Poisson equations [16,17] were developed to study deviations from the Z_b^2 scaling law. Here a scaling of the stopping power close to $Z_b^{1.5}$ was found for low beam velocities.

The aim of this paper is to treat beam-plasma coupling effects in the stopping power using quantum kinetic theory. In particular, we extend the energy loss calculations presented in Ref. [18] to the case of ion beams with a given ion charge number Z_b. A *T*-matrix approach (binary collision approximation) including dynamic screening effects is applied to study strong correlations between the beam ions and the quantum plasma.

The paper is organized as follows. In Sec. II we briefly recall our approach to give the basic expressions for the stopping power for ion beams in dense plasmas. The ion charge number dependence of the stopping power is investigated in Sec. III. Finally, comparisons of our results with data obtained from numerical simulations are given.

II. STOPPING POWER OF STRONGLY CORRELATED PLASMAS

In the frame of kinetic theory, the energy loss of a particle beam in a plasma can be characterized by the time derivative of the mean kinetic energy of the beam particles or by the time derivative of the average x component of the beam particle momentum (the x direction is considered to be parallel to the beam velocity $\boldsymbol{v}$). With the latter definition, the stopping power, i.e., the energy loss per unit length, is given by

$$\frac{\partial}{\partial x}\langle E\rangle=\frac{1}{n_b}\int\frac{d\boldsymbol{p}}{(2\pi\hbar)^3}\frac{\boldsymbol{p}\cdot\boldsymbol{v}}{v}\frac{\partial}{\partial t}f_b(\boldsymbol{p},t). \tag{3}$$

We determine the beam particle distribution function $f_b(\boldsymbol{p},t)$, from a quantum kinetic equation which is used in the Markovian form, i.e., retardation effects are neglected [19]. For a homogeneous plasma without external fields, the kinetic equation can be written as $\partial f_b/\partial t=\Sigma_c I_{bc}$, where the collision terms I_{bc} describe the interaction between the beam particles and the species of the target plasma. There exist different schemes of approximations in many particle theory to model the beam-plasma interaction. A first important one is the polarization approximation leading to the Lenard-Balescu kinetic equation [20,21]. The latter can be applied to weakly interacting particles using the dielectric function in the RPA. On the other hand, the quantum Boltzmann equation can be obtained by applying the binary collision approximation [22,23]. This scheme allows one to include strong beam-plasma coupling effects in the framework of the T-matrix approach describing the two-body interaction by the statically screened Coulomb (Debye) potential.

Considering a sharply peaked beam particle distribution function $f_b(\boldsymbol{p},t)\sim\delta(\boldsymbol{p}-m_b\boldsymbol{v})$ and using the Boltzmann kinetic equation for a nondegenerate, fully ionized quantum plasma, from Eq. (3) we obtain

$$\frac{\partial}{\partial x}\langle E\rangle=\frac{1}{(2\pi)^2\hbar^3}\sum_c\frac{m_c^2}{m_{bc}^3}\frac{n_c\Lambda_c^3}{v}k_BT\int_0^\infty dp\,p^3Q_{bc}^T(p)$$
$$\times\left\{\left(1-\frac{m_{bc}k_BT}{m_cp}\right)e^{-m_c/2k_BT[(p/m_{bc})-v]^2}+\left(1+\frac{m_{bc}k_BT}{m_cp}\right)e^{-m_c/2k_BT[(p/m_{bc})+v]^2}\right\}. \tag{4}$$

Here the sum runs over all plasma species, $m_{bc}=m_bm_c/(m_b+m_c)$ is the reduced mass, p denotes the modulo of the momentum of relative motion between beam and plasma particles, and $\Lambda_c=(2\pi\hbar^2/k_BTm_c)^{1/2}$ is the thermal wavelength. If the beam particles are much heavier than the plasma particles, the relation $v\,\partial\langle E\rangle/\partial x=\partial\langle E\rangle/\partial t$ can be applied to obtain the corresponding energy loss per unit time except for very low beam velocities.

The main input quantity in expression (4) is the transport cross section Q_{bc}^T which is defined as $Q_{bc}^T(p)=2\pi\int_0^\pi(1-\cos\vartheta)\sigma_{bc}(p,\vartheta)d\vartheta$, where ϑ is the scattering angle. The differential cross section σ_{bc} is related to the retarded T matrix according to $\sigma_{bc}(p,\vartheta)\sim|\langle\boldsymbol{p}|T_{bc}^R(\omega)|\overline{\boldsymbol{p}}\rangle|^2$. Here the energy argument of the T matrix is on the energy shell, i.e., $\omega=E(p)+E(\overline{p})+i\epsilon$ with the single particle energy $E(p)$. Furthermore, $\boldsymbol{p}$ and $\overline{\boldsymbol{p}}$ are the momenta of relative motion before and after the collision, respectively. The retarded T matrix is determined by the Lippmann–Schwinger equation. Using an operator notation, this equation can be written as

$$T_{bc}^R(\omega)=V_{bc}^S+V_{bc}^S\frac{1}{(\omega-H_{bc}^0+i\epsilon)}T_{bc}^R(\omega), \tag{5}$$

where V_{bc}^S denotes the statically screened Coulomb potential, and H_{bc}^0 is the free two particle Hamiltonian. In lowest order perturbation theory, the T matrix is given by the first term on the right-hand side of Eq. (5), i.e., $T_{bc}^S=V_{bc}^S$. In this case, we obtain the transport cross section in first Born approximation

$$Q_{bc}^T(p)=\frac{2\pi\hbar^4Z_b^2}{p^4a_B^2}\left[\ln(1+4z)-\frac{4z}{1+4z}\right], \tag{6}$$

with the abbreviation $z=p^2/\hbar^2\kappa^2$ and the Bohr radius $a_B=\hbar^2/e^2m_{bc}$. In order to describe the two-particle scattering problem without restrictions with respect to the coupling strength, the full T matrix has to be calculated. This can be done, e.g., by matrix inversion of Eq. (5). In the considered nondegenerate case, it is more appropriate to use the scattering phase shift technique. Then for the transport cross section we obtain

$$Q^T(p)=\frac{4\pi\hbar^2}{p^2}\sum_{l=0}^\infty(l+1)\sin^2(\eta_l-\eta_{l+1}). \tag{7}$$

The scattering phase shifts η_l follow from numerical solution of the radial Schrödinger equation which corresponds to the determination of the full T matrix [18].

Using the cross section determined by Eq. (7) in expression (4), strong coupling effects in the beam-plasma interaction are taken into account. But collective effects such as

plasma oscillations are not included. The reason for this is that the screening is treated in the static limit. Therefore, at high beam velocities, the stopping power cannot be described correctly by formula (4) because dynamic screening is of importance in that range. Dynamic screening effects can be included if the stopping power is considered in a dynamically screened first Born approximation. The latter follows by inserting the collision integral of the quantum Lenard-Balescu equation into Eq. (3) [25,26]:

$$\frac{\partial}{\partial x}\langle E\rangle = \frac{2Z_b^2 e^2}{\pi v^2}\int_0^\infty \frac{dk}{k}\int_{(\hbar k^2/2m_b)-kv}^{(\hbar k^2/2m_b)+kv} d\omega \times\left[\omega-\frac{\hbar k^2}{2m_b}\right]\mathrm{Im}\,\varepsilon_{\mathrm{RPA}}^{-1}(k,\omega)n_B(\omega). \tag{8}$$

Here the stopping power is given in terms of the imaginary part of the inverse dielectric function $\varepsilon_{\mathrm{RPA}}$ which was used in the RPA and the Bose distribution function of the plasmons $n_B=[\exp(\hbar\omega/k_BT)-1]^{-1}$.

We see that expression (8) represents a quantum mechanical generalization of the stopping power formulas derived in the framework of dielectric theory [7] or from the linearized classical Vlassow equation [17]. It allows one to describe collective effects relevant at high beam velocities, but its validity is restricted to weakly interacting particles.

To include both dynamic screening effects and close collisions, an ansatz according to Gould and DeWitt [24] can be used. For the stopping power, the scheme reads [18]

$$\frac{\partial}{\partial x}\langle E\rangle = \frac{\partial}{\partial x}\langle E\rangle_{T\ \mathrm{matrix}}^{\mathrm{static}} + \frac{\partial}{\partial x}\langle E\rangle_{\mathrm{Born}}^{\mathrm{dynamic}} - \frac{\partial}{\partial x}\langle E\rangle_{\mathrm{Born}}^{\mathrm{static}}. \tag{9}$$

In this combined model, the stopping power is determined by the sum of the T matrix and the dynamic RPA expressions subtracting the static first Born term to avoid double counting. The result is a T-matrix approach for the stopping power given by a dynamically screened first Born approximation and statically screened higher order ladder terms. In this way, screening is described in a linear approximation which corresponds to the level of the linearized Vlassow equation. However, in contrast to the Vlassow-Poisson scheme, strong binary collisions are taken into account by the T-matrix contributions beyond the first Born approximation contained in the first term of Eq. (9).

For high beam velocities, the well-known Bethe-type asymptotic expression follows from the combined model

$$\lim_{v\to\infty}\frac{\partial}{\partial x}\langle E\rangle = -\frac{Z_b^2 e^2\omega_{\mathrm{pl}}^2}{v^2}\ln\left(\frac{2m_e v^2}{\hbar\omega_{\mathrm{pl}}}\right), \tag{10}$$

with $\omega_{\mathrm{pl}}=(4\pi e^2\Sigma_c n_c/m_c)^{1/2}$ being the plasma frequency. As the T-matrix and static Born approximations of the stopping power coincide for high beam velocities, this expression is equal to the asymptotic formula following from Eq. (8). The asymptotic expression (10) was successfully used to describe the stopping of ion beams in the high velocity region; see, e.g., [27,28].

To demonstrate the effects included in the different approximation schemes presented above, we plotted the stopping power for a proton beam in an electron gas in Fig. 1. All curves show the same general behavior: a linear increase for low beam velocities and, after a maximum, a decrease according to $\partial\langle E\rangle/\partial x\sim \ln(v)/v^2$ for high beam velocities. Multiple scattering included in the T-matrix approach reduces the stopping power for low and intermediate beam velocities. Furthermore, for low beam velocities, dynamic screening effects are negligible. Here the static and dynamic Born approximations coincide and, therefore, the (static) T matrix and the combined model give the same result. On the other hand, the weak coupling approximation is sufficient for high beam velocities. In this case, the dynamic expressions (8) and (9) give results two times larger than the static Born and T-matrix approximations. Therefore, the combined model interpolates between the two limiting cases: the static T matrix for low beam velocities and the dynamic RPA results for high beam velocities.

III. Z DEPENDENCE OF THE STOPPING POWER

The dependence of the stopping power on the beam ion charge number Z_b is an essential problem to understand the beam-plasma interaction. All standard approaches for the stopping power, e.g., the dielectric response theory and the simple Bethe formula [29], predict an increase of the stopping power according to a Z_b^2 scaling law. The dynamic and the static Born approximations show similar behaviors. The reason for this is that these theories consider the beam-plasma interaction in the weak coupling limit, which gives exact results only for high temperature plasmas, sufficiently low ion charges, and/or high beam velocities.

Of course, this behavior changes for strong beam-plasma coupling. As already mentioned, the T matrix determined by the Lippmann-Schwinger equation (5) accounts for strong correlation effects. The Z_b^2 scaling law follows if only the first term on the right-hand side of Eq. (5) is used, i.e., $\sigma_{ab}\sim|V_{ab}^S|^2$. However, for strong beam-plasma coupling, one has to go beyond the first Born approximation, summing up the higher order ladder terms included in the second right-hand side term of Eq. (5). Now the ion-electron interaction

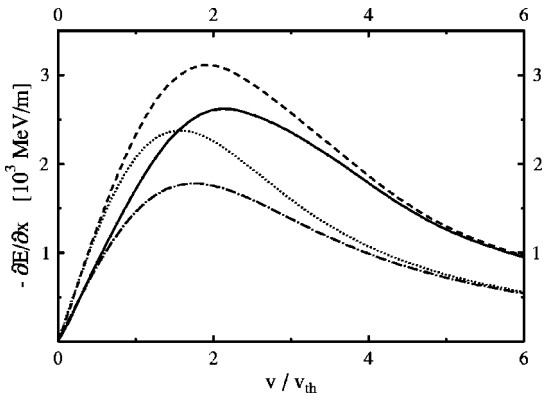

FIG. 1. Stopping power for a proton beam in an electron gas versus beam velocity (in units of the thermal velocity $v_{\mathrm{th}}=\sqrt{k_BT/m_e}$). The electron density and temperature are $n=10^{21}$ cm^{-3} and $T=5\times10^4$ K, respectively. The applied approximations are the RPA (dashed line), the static Born approximation (dotted line), the static T-matrix approximation (dash-dotted line), and the combined scheme (full line).

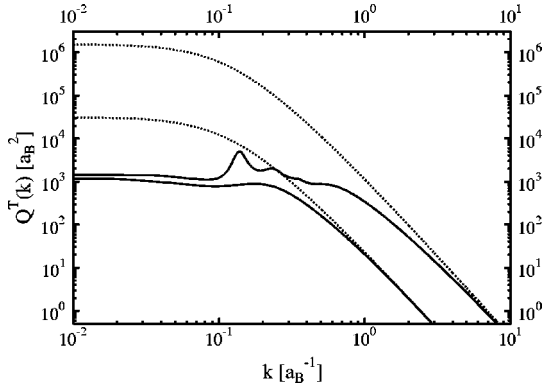

FIG. 2. Transport cross section $Q^T(k)$ vs wave number of the relative motion $k=p/\hbar$ for ion-electron scattering in the static Born (dotted line) and T-matrix (full line) approximations. The ion charge number is $Z_b=7$ for the upper pair of lines and $Z_b=1$ for the lower one. The inverse screening length is $\kappa=0.1a_B^{-1}$.

potential enters the cross sections in a nonlinear way leading to deviations from the Z_b^2 scaling. Here we want to mention that the two-particle interaction is approximated by the statically screened Coulomb (Debye) potential. This means that the deviations from the Z_b^2 scaling obtained from our approach are not an effect of nonlinear screening but an effect of multiple scattering included in the T matrix and, therefore, an effect of a more exact treatment of the two-particle scattering as compared to the Born approximation.

First, we demonstrate the influence of T-matrix effects on the scattering quantities. In Fig. 2, the transport cross section is plotted versus wave number of relative motion $k=p/\hbar$ in static T-matrix and Born approximations. While for large wave numbers both approximations approach each other, the higher order ladder terms included in the T matrix reduce the cross section for small k values. These deviations increase with increasing ion charge number. The low energy peaks in the T-matrix cross sections are due to resonance states in ion-electron scattering. These resonances are typical quantum effects describing the contribution of former bound states which are merged into the continuum by pressure ionization (Mott effect) [30].

Let us focus on the T-matrix effects in the stopping power now. In Fig. 3, the stopping power in the static T-matrix and Born approximations is shown versus beam velocity for three values of the ion charge number. In all cases, one can observe a reduction of the stopping power in the T-matrix approximation compared to the Born result. While for single charged ions only small deviations between the applied models occur, they increase for the higher ion charge numbers and can be observed up to higher beam velocities.

The normalized stopping power $\partial\langle E\rangle/\partial x/Z_b^2$ versus ion charge number is shown in Fig. 4 for two plasma densities. Due to the small beam velocity ($v=0.2\ v_{\rm th}$), the results for static and dynamic screening coincide. Again, one observes that the T-matrix approach causes a reduction of the stopping power. This effect increases with increasing coupling strength, i.e., for higher ion charge numbers and higher plasma densities. Additionally, it is clearly visible that the T-matrix data cannot be fitted by a Z_b^2 scaling law in contrast to the weak coupling approximations (dashed lines).

To give an estimate of strong beam-plasma coupling effects over a wide range of plasma parameters, the exponent of a Z_b^x scaling ($\partial\langle E\rangle/\partial x|_{Z_b=x}=Z_b^x\ \partial\langle E\rangle/\partial x|_{Z_b=1}$) valid for the low velocity range is given in Table I. For very hot plasmas and small Z_b, the scaling is close to Z_b^2. But if the beam-plasma coupling increases, i.e., the Coulomb parameter approaches $\eta=1$ or is larger, significant deviations from this scaling can be found. Here, the scaling exponent varies in the range of $x=1.3$–1.9. Obviously, it is larger for higher temperatures and decreases with increasing plasma density and beam charge number. These results are in good agreement with the scaling, which was found experimentally in electron cooling devices [5,9].

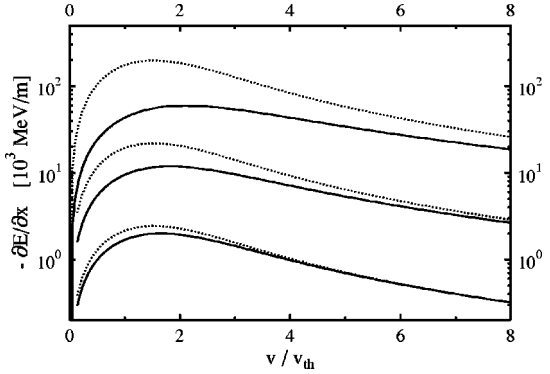

FIG. 3. Stopping power for a heavy ion beam in an electron gas with $n=1.7\times10^{21}$ cm^{-3} and $T=10^5$ K vs beam velocity ($v_{\rm th}=\sqrt{k_BT/m_e}$ is the thermal velocity). The ion charge numbers are $Z_b=9$ (upper pair), $Z_b=3$ (pair in the middle), and $Z_b=1$ (lower pair). The applied models are the static Born (dotted line) and the static T-matrix (full line) approximations.

IV. COMPARISON WITH NUMERICAL SIMULATION DATA

Now we compare our results for the stopping power calculated from quantum kinetic equations with data obtained from classical particle in cell (PIC) and molecular dynamics (MD) simulations which were performed by Zwicknagel and co-workers [6,14,15]. The calculations were done with typically 10^3 particles per cell for the MD simulations, and 10^5

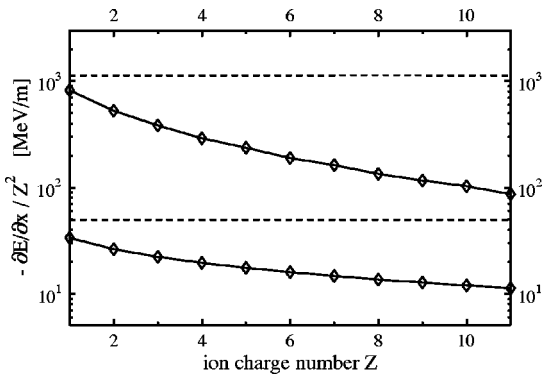

FIG. 4. Normalized stopping power for an ion beam in an electron gas with $n=3.4\times10^{21}$ cm^{-3} and $T=5\times10^4$ K (upper lines) and $n=3.4\times10^{19}$ cm^{-3} and $T=5\times10^4$ K (lower lines) versus ion charge number Z_b. The beam velocity is $v=0.2\ v_{\rm th}$. The line styles correspond to the Born (dashed lines) and the T-matrix approximations (full lines).

TABLE I. Scaling of the stopping power for low beam velocities. Exponent x of the Z_b^x scaling ($\partial\langle E\rangle/\partial x|_{Z_b=x} = Z_b^x \times \partial\langle E\rangle/\partial x|_{Z_b=1}$) for different plasma temperatures, plasma densities, and beam charge numbers.

n (cm^{-3})	T (K)	Γ	$\eta_{Z=1}$	$x_{Z=2}$	$x_{Z=5}$	$x_{Z=8}$	$x_{Z=11}$
6.8×10^{21}	10^7	0.005	0.18	1.98	1.94	1.92	1.91
6.8×10^{20}	10^6	0.024	0.56	1.87	1.82	1.80	1.79
1.7×10^{24}	10^6	0.32	0.56	1.83	1.67	1.60	1.54
1.7×10^{19}	10^5	0.069	1.78	1.74	1.70	1.68	1.67
6.8×10^{19}	10^5	0.11	1.78	1.70	1.66	1.63	1.62
1.7×10^{18}	10^4	0.32	5.62	1.54	1.48	1.44	1.41
6.8×10^{18}	10^4	0.51	5.62	1.45	1.36	1.30	1.26

test particles for the PIC simulations. Special account was paid for an adequate description of close collisions. Therefore, (i) the usual PIC technique was modified to include collisions, and (ii) an adaptive time step control for subclusters of particles was introduced to treat strong Coulomb interactions. For a more detailed description of the simulation techniques, we refer to Ref. [6].

First, let us consider the case of a weakly coupled target plasma. In Figs. 5 and 6, the reduced stopping power $(\partial\langle E\rangle/\partial x)/Z_b^2\Gamma^3$ is shown as a function of the beam velocity for two values of the beam-plasma coupling parameter, $Z_b\Gamma^{3/2}=0.12$ and 0.354. It should be noted that essential contributions coming from quantum corrections are not expected for the parameters considered in these figures. The curves give the stopping power following from the different approximations to treat the beam-plasma interaction in the kinetic equation as described in Sec. II. Data from PIC simulations [31,15] are added. The results shown in Fig. 5 are calculated for a beam ion charge number $Z_b=5$. At low beam velocities $v<v_{\rm th}$, both the static and dynamic T-matrix results agree well with the simulation data. On the other hand, considerable deviations are observed between the simulations and the results obtained from the weak coupling theories (static and dynamic first Born approximations). For beam velocities higher than the electron thermal velocity up to $v\leqslant 3v_{\rm th}$, only the combined T-matrix model including dynamic screening leads to a reasonable agreement with the simulation data. This confirms the expected result that both strong collisions and dynamic screening effects determine the stopping power for moderate velocities. As already outlined in Sec. II, at high beam velocities, the combined T-matrix model approaches the dynamic Born approximation with the well-known asymptotics given by formula (10). This behavior is not reproduced by the simulations, which tend to give slightly smaller results at high beam velocities. We found that in this classical region the T-matrix results show, similar to the PIC simulation data, a dependence only on the parameter $Z_b\Gamma^{3/2}$ if the stopping power and the beam velocity are given in thermal units ($k_BT/l, v_{\rm th}$). Such behavior cannot be found if weak coupling theories are applied because there exists no classical limit in this case.

In Fig. 6, stopping power results are shown for $Z_b=10$ and $\Gamma=0.1$. Similar to Fig. 5, the weak coupling theories overestimate the stopping power in the low and moderate velocity ranges. Again, a good agreement between the PIC data and the T-matrix results is found for beam velocities below $v_{\rm th}$. This agreement is extended slightly to higher velocities using the combined model which includes dynamic screening effects. But deviations can already be observed for $v>2v_{\rm th}$. Here, one has to remember the fact that dynamic screening is accounted for in the weak coupling

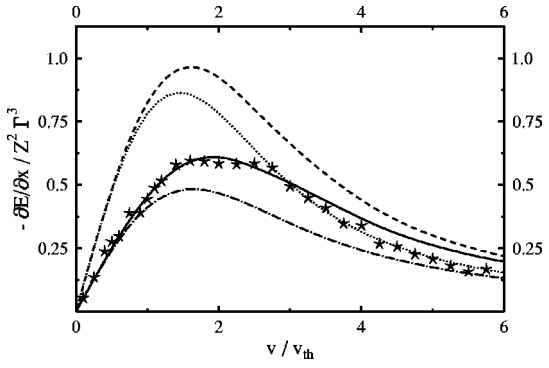

FIG. 5. Comparison of the different approximation schemes (RPA—dashed line; static Born—dotted line; static T matrix—dash-dotted line; combined scheme—full line) for the stopping power with data from PIC simulations (stars). The data describe an ion beam with a charge number of $Z_b=5$ moving in an electron gas with $n=1.1\times10^{20}$ cm^{-3} and $T=1.6\times10^5$ K ($Z_b\Gamma^{3/2}=0.12$). The stopping power $\partial\langle E\rangle/\partial x$ is given in thermal units, i.e., $3k_BT/l$ ($l=e^2/k_BT$ is the Landau length) and is plotted vs beam velocity ($v_{\rm th}=\sqrt{k_B,T/m_e}$).

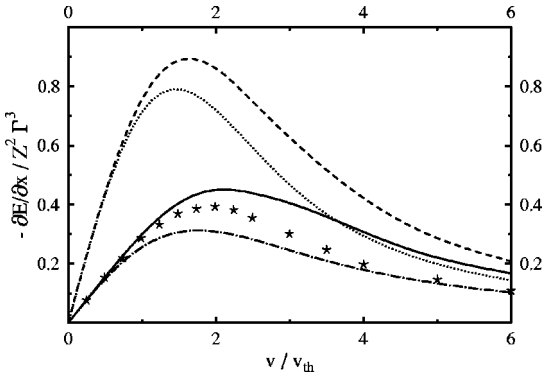

FIG. 6. Comparison of the different approximation schemes (line styles same as in Fig. 5) for the stopping power with data from PIC simulations (stars). The data describe an ion beam with a charge number of $Z_b=10$ moving in an electron gas with $n=1.4\times10^{20}$ cm^{-3} and $T=1.3\times10^5$ K ($Z_b\Gamma^{3/2}=0.354$). The stopping power is given in thermal units (see Fig. 5).

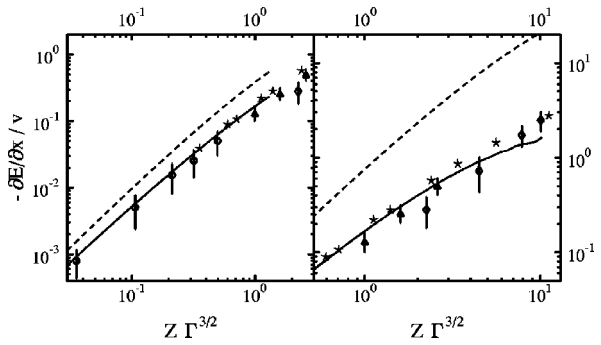

FIG. 7. Friction coefficient $\partial\langle E\rangle/\partial x/v$ vs parameter $Z_b\Gamma^{3/2}$ for an ion beam with $Z_b=10$. The stopping power and beam velocity are given in thermal units (see Fig. 5). The electron plasma temperatures are $T=10^6$ K (left figure) and $T=5\times10^4$ K (right figure). The data correspond to the Born (dotted line) and *T*-matrix (full line) approximations. For comparison, results from classical molecular dynamics [$\Gamma=0.11$ (circles), $\Gamma=0.34$ (diamonds), and $\Gamma=1.08$ (triangles)] and PIC (stars) simulations are given.

limit only. For moderate beam velocities, nonlinear dynamic screening effects are also expected to be significant. The nonlinear coupling effects included in our approach are due to statically screened higher order ladder diagrams of the *T* matrix.

Of course, strong beam-plasma correlations are most important for low beam velocities where the stopping power depends linearly on v. Therefore, the friction coefficient $(\partial\langle E\rangle/\partial x)/v$ is of special interest to check the relevance of strong coupling effects. As already discussed, the dynamics of screening is of minor importance in this low velocity range. Therefore, it is justified to use the stopping power data calculated from kinetic equations assuming statically screened Coulomb interactions. Results for the friction coefficient in Born and *T*-matrix approximations are plotted in Fig. 7 versus the parameter $Z_b\Gamma^{3/2}$ for two temperatures $T=10^6$ K (left) and $T=5\times10^4$ K (right). In both cases, the beam ion charge number was chosen to be $Z_b=10$, and a comparison with data obtained from PIC and MD simulations [15] is given. A good agreement between the *T*-matrix results and the simulation data can be observed over the whole parameter range in the high temperature case. The Born curve slightly overestimates the friction coefficient. These deviations increase if lower temperatures are considered, as shown in the right part of Fig. 7. In the latter case, the friction coefficient calculated in the *T*-matrix approximation agrees well up to coupling parameters $Z_b\Gamma^{3/2}\leqslant4$. For higher coupling parameters the *T*-matrix approach gives smaller values compared to the simulation data. Here one enters the region where quantum effects are of importance. It turns out that for the given temperature and beam charge number, the parameter $\kappa\lambda$ increases from $\kappa\lambda=0.3$ ($Z_b\Gamma^{3/2}=4$) up to $\kappa\lambda=0.7$ ($Z_b\Gamma^{3/2}=10$). But only for $\kappa\lambda\ll1$ is the trajectory of the beam particle well defined during the scattering process, and, therefore, classical calculations like MD and PIC simulations are questionable in this region. With increasing values of the parameter $Z_b\Gamma^{3/2}$, i.e., increasing plasma density, the influence of quantum diffraction effects leads to a further reduction of the friction coefficient compared to the classical simulation data (phase space occupation effects are negligible for the plotted plasma parameters). For the same plasma parameters, similar reductions can also be found for other beam charge numbers. This shows the relevance of including quantum corrections in the calculation of the stopping power for low beam velocities in the region of strongly coupled plasmas.

Of course, the kinetic approach used to determine the stopping power in the strong coupling regime requires further improvements based on quantum many particle theory. Instead of the combined scheme given by Eq. (9), where dynamic screening is accounted for in the first Born term only, one should start rigorously from a screened ladder approximation including dynamic screening in the higher order ladder terms too [32]. Furthermore, the screened two-body potential should be evaluated beyond the RPA in the way that both multiple scattering and nonlinear screening effects are described.

If the target plasma is partially ionized, the stopping power is determined not only by the free plasma particles but also by the bound states. Here strong coupling effects such as in-medium ionization and excitation processes, the lowering of the ionization energy and the Mott effect have to be taken into account [33,34]. Furthermore, beam stripping and electron capture processes have to be included to describe the charge state evolution of the projectile ions which can be of special importance for the stopping power [35].

ACKNOWLEDGMENTS

The authors would like to thank G. Zwicknagel for fruitful discussions, and for providing simulation data. This work was supported by the Deutsche Forschungsgemeinschaft SFB 198 ''Kinetik partiell ionisierter Plasmen.''

[1] R. Bock, I. Hoffmann, and R. Arnold, Nucl. Sci. Appl. **2**, 97 (1984).
[2] C. Deutsch, Ann. Phys. (Paris) **11**, 1 (1986).
[3] For a recent overview see *Proceedings of the International Symposium on Heavy Ion Inertial Fusion* (Heidelberg, 1997), edited by I. Hoffmann and H.J. Bluhm [Nucl. Instrum. Methods Phys. Res. A **415** (1998)].
[4] K.-G. Dietrich, D.H.H. Hoffmann, E. Boggasch, J. Jacoby, H. Wahl, M. Elfers, C.R. Haas, V.P. Dubenkov, and A.A. Golubev, Phys. Rev. Lett. **69**, 3623 (1992).
[5] Th. Winkler, K. Bechert, F. Bosch, H. Eickhoff, B. Franzke, F. Nolden, H. Reich, B. Schlitt, and M. Steck, Nucl. Instrum. Methods Phys. Res. A **391**, 12 (1997).
[6] G. Zwicknagel, C. Toepffer, and P.-G. Reinhard, Phys. Rep. **309**, 117 (1999).
[7] J. Lindhard, K. Dan. Vidensk. Selsk. Mat. Fys. Medd. **28**, 8 (1954).
[8] W.H. Barkas, N.J. Dyer, and H.H. Heckmann, Phys. Rev. Lett. **11**, 26 (1963).
[9] A. Wolf, C. Ellert, M. Grieser, D. Habs, B. Hchadel, R. Repnow, and D. Schwalm, in *Beam Cooling and Related Topics*, edited by J. Bosser (CERN, Genf, 1994).

[10] J.M. Pitarke, R.H. Ritchie, P.M. Echenique, and E. Zaremba, Europhys. Lett. **24**, 613 (1993).
[11] I. Nagy, A. Arnau, and P.M. Echenique, Phys. Rev. A **40**, 987 (1989).
[12] E. Zaremba, A. Arnau, and P.M. Echenique, Nucl. Instrum. Methods Phys. Res. B **96**, 619 (1996).
[13] J.W. Dufty, M. Berkovsky, Nucl. Instrum. Methods Phys. Res. B **96**, 626 (1995).
[14] G. Zwicknagel, D. Klakow, P.-G. Reinhard, and C. Toeppfer, Contrib. Plasma Phys. **33**, 395 (1993).
[15] G. Zwicknagel, C. Toeppfer, and P.-G. Reinhard, Fusion Eng. Des. **32-33**, 523 (1996).
[16] O. Boine-Frankenheim, Phys. Plasmas **3**, 1585 (1996).
[17] Th. Peter and J. Meyer-ter-Vehn, Phys. Rev. A **43**, 1998 (1991).
[18] D.O. Gericke, M. Schlanges, and W.D. Kraeft, Phys. Lett. A **222**, 241 (1996).
[19] For a discussion of non-Markovian effects in kinetic equations, we refer to D. Kremp, M. Bonitz, W.D. Kraeft, and M. Schlanges, Ann. Phys. (N.Y.) **258**, 320 (1997).
[20] D.F. DuBois, in *Lectures in Theoretical Physics*, edited by W.E. Brittin (Gordon and Beach, New York, 1967), Vol. IX C.
[21] Y.L. Klimontovich, *Kinetic Theory of Nonideal Gases and Nonideal Plasmas* (Pergamon Press, Oxford, 1982).
[22] P. Danielewicz, Ann. Phys. (N.Y.) **152**, 239 (1984).
[23] D. Kremp, M. Schlanges, and Th. Bornath, J. Stat. Phys. **41**, 661 (1985).
[24] W.D. Kraeft and B. Strege, Physica A **149**, 313 (1988).
[25] K. Morawetz and G. Röpke, Phys. Rev. E **54**, 4134 (1996).
[26] H.A. Gould, H.E. DeWitt, Phys. Rev. **155**, 68 (1967).
[27] D.H.H. Hoffmann, K. Weyrich, H. Wahl, D. Gardés, R. Bimbot, C. Fleurier, Phys. Rev. A **42**, 2313 (1990).
[28] A. Golubev, M. Basko, A. Fertman, A. Kozodaev, N. Mesheryakov, B. Sharkov, A. Vishnevskiy, V. Fortov, M. Kulish, V. Gryaznov, V. Mintsev, E. Golubev, A. Pukhov, V. Smirnov, U. Funk, S. Stoeve, M. Stetter, H.-P. Flierl, D.H.H. Hoffmann, J. Jakobi, and I. Iosilevski, Phys. Rev. E **57**, 3363 (1998).
[29] H. Bethe, Ann. Phys. (Leipzig) **5**, 325 (1930).
[30] W.D. Kraeft, D. Kremp, W. Ebeling, and G. Röpke, *Quantum Statistics of Charged Particle Systems* (Akademie-Verlag, Berlin, 1986).
[31] G. Zwicknagel (private communication).
[32] First attempts to derive dynamically screened ladder equations for nonequilibrium systems in the frame of Green's function techniques are given in W. Schäfer, R. Binder, and K.H. Schuldt, Z. Phys. B **70**, 145 (1988); D. Kremp, W.D. Kraeft, and M. Schlanges, in *Strongly Coupled Coulomb Systems*, edited by G.J. Kalman, J.M. Rommel, and K. Blagoev (Plenum Press, New York, 1998).
[33] M. Schlanges, D.O. Gericke, W.D. Kraeft, and Th. Bornath, Nucl. Instrum. Methods Phys. Res. A **415**, 517 (1998).
[34] M. Schlanges and Th. Bornath, Physica A **192**, 262 (1993); Th. Bornath and M. Schlanges, Physica A **196**, 427 (1993).
[35] Th. Peter and J. Meyer-ter-Vehn, Phys. Rev. A **43**, 2015 (1991).